Low-Energy (5–120 eV) Electron-Stimulated Dissociation of Amorphous D_2O Ice: $D(^2S)$, $O(^3P_{2,1,0})$, and $O(^1D_2)$ Yields and Velocity Distributions

Greg A. Kimmel and Thomas M. Orlando*

Environmental Molecular Sciences Laboratory, Pacific Northwest Laboratory, Richland, Washington 99352

(Received 1 May 1995)

Laser resonance enhanced multiphonon ionization spectroscopy was used to measure yields and velocity distributions of the $D(^2S)$, $O(^3P_{2,1,0})$, and $O(^1D_2)$ produced during low-energy (5–120 eV) electron-beam irradiation of amorphous D_2O ice. Electron-stimulated dissociation has a very low energy threshold (~6–7 eV), and the neutral fragments desorb with low kinetic energies (~60–85 meV) which are *independent* of the incident electron energy. The data suggest that desorption of neutral fragments results from dissociation of excited states formed directly or via electron-ion recombination.

PACS numbers: 79.20.Kz, 33.80.Rv, 34.80.Gs

The structure of condensed water [1,2] and its interactions with electrons [3–6], photons [7,8], and ions [9,10] have been extensively studied due to its importance in many areas of science. Although the role of excited states, dissociative electron attachment, electron-ion recombination, and exciton dissociation have been discussed, there is no consensus regarding the mechanisms of stimulated dissociation or desorption in ice and molecular solids in general. Studies using laser resonance enhanced multiphonon ionization (REMPI) detection of neutral desorbates have demonstrated the importance of valence-level excitations in electron-stimulated desorption (ESD) from (sub)monolayer adsorbate layers on metal surfaces [11,12]. Some of the more recent ESD studies of molecular solids report neutral yields [5], neutral velocity distributions [13], and metastable yields [14]. Although detailed information on the nature of the excited states and the potential energy surfaces involved in ESD can be obtained from measurements of desorbate quantum-state distributions and desorption threshold energies, none of the state-resolved EDS studies reported thus far have investigated molecular solids.

This Letter reports the first quantum-state-resolved study of low-energy electron-stimulated interactions in amorphous ice. We utilize REMPI spectroscopy to monitor the desorption threshold energies, yields, and velocity distributions of the $D(^2S)$, $O(^3P_{2,1,0})$, and $O(^1D_2)$ desorbates produced during electron-beam irradiation of thin films (~200 Å) of amorphous D_2O ice. We find that (1) the $D(^2S)$, $O(^3P_{2,1,0})$, and $O(^1D_2)$ have the same low desorption threshold of ~6–7 eV, (2) these neutral fragments desorb with low velocities, (3) the shapes of the velocity distributions are *independent* of the excitation energy over the entire energy range investigated (5–120 eV), and (4) the $D(^2S)$ yield is proportional to the total excitation cross section for the incident electrons. The evidence suggests that desorption of neutral fragments results from the dissociation of the neutral excited states (excitons) which are formed via either direct electronic excitation or electron-ion recombination. These single-electron final states are quire different from the multihole final states invoked to explain the ESD of protons from amorphous ice [4,15].

The experiments were performed in an ultrahigh vacuum ($\sim 1 \times 10^{-10}$ Torr) system which has been described previously [5,6]. All the experiments were done on a liquid nitrogen cooled Pt(111) crystal at $T_s = 88$ K. D_2O multilayers (~200 Å) were prepared under conditions that have been shown to produce amorphous ice [2]. The ice samples were irradiated with a variable pulsed (200 nsec–25 μsec) electron beam, and the neutral atomic fragments desorbing from the surface were detected using REMPI spectroscopy. The electron beam had an energy spread of ~0.3 eV, a typical current density of $\sim 10^{10}$ electrons/cm^2 pulse, and a beam spot size of ~1.5 mm. The low incident electron flux resulted in negligible heating of the ice layer. The $D(^2S)$, $O(^3P_J)$, and $O(^1D_2)$ signals were independent of total electron dose, and the signals varied linearly as a function of incident electron current. Since the sublimation rate for amorphous ice is quite low at 88 K, thermal desorption did not influence any of the results. In addition, the electron-stimulated neutral desorbate yields were low enough to preclude any secondary (above the surface) interactions.

The neutral state-specific detection schemes involved (2 + 1) REMPI transitions. The two-photon transitions used for detecting the $D(^2S)$, $O(^3P_{J=2,1,0})$, and $O(^1D_2)$ were the $3s\,^2S \leftarrow 1s\,^2S$ at 205.1 nm, $3p\,^3P_{2,1,0} \leftarrow 2p\,^3P_{2,1,0}$ at 225.7–226.2 nm, and $3p\,^1F_3 \leftarrow {}^1D_2$ at 203.8 nm, respectively. The laser wavelengths necessary for these detection schemes were generated by frequency tripling the output of a Nd:YAG pumped dye laser with KDP-C and β-barium borate crystals. Typical laser pulse powers were ~0.5–1.5 mJ/pulse, and our estimated detection efficiencies were $\sim 10^{5-6}$ atoms/[cm^3(quantum state)]. All experiments were done in the time-of-flight (TOF) mode in which the neutrals produced by the pulsed electron beam were resonantly ionized ~4 mm above the surface by the focused laser beam. State-specific TOF distributions were obtained by varying the delay time between the electron-beam pulse and the laser pulse.

 0031-9007/95/75(13)/2606(4)$06.00

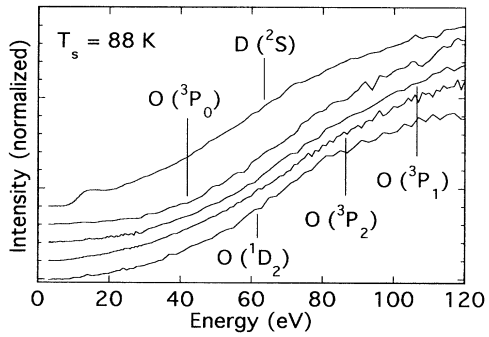

FIG. 1. Intensity vs electron energy for $D(^2S)$, $O(^3P_{J=2,1,0})$, and $O(^1D_2)$. The intensities were measured using relatively long (15–25 μsec) electron-beam pulses which integrate the entire TOF distributions (see Fig. 3). The curves, which have been normalized and offset for clarity, are the average of several measurements for each species. The scatter in the data is indicative of the error.

The $D(^2S)$, $O(^3P_{J=2,1,0})$, and $O(^1D_2)$ yields versus incident electron energy E_i are shown in Fig. 1. The spectra were obtained using electron-beam pulse widths (15 and 25 μsec for the D and O atoms, respectively) which effectively integrate the entire velocity distributions. The $D(^2S)$ has an apparent threshold at ~6.5 eV (Fig. 2), which is well below the 21 eV threshold reported for ESD of H^+ from ice [4]. Above threshold, the $D(^2S)$ intensity increase rapidly until a distinct plateau is reached for $\sim 14 \leq E_i \leq 21$ eV. The signal increases more gradually for electron energies above ~21 eV. The thresholds for the $O(^3P_2)$ and $O(^1D_2)$ signals are $E_{th} \sim 6$–7 eV (Fig. 2). The O atom intensities versus energy are all similar (Fig. 1), suggesting that the electronically excited $O(^1D_2)$ results from the same process which produces ground state $O(^3P_J)$. The shape of the intensity versus energy curves for the O atoms are somewhat different than that of the $D(^2S)$. In particular, at 88 K, the distinctive plateau, which is observed in the $D(^2S)$ yield from ~14 to 21 eV, is not observed in either the $O(^3P_2)$ or $O(^1D_2)$ curves. Above 21 eV, the O atom intensities increase more rapidly with electron energy than the $D(^2S)$.

Figure 3 shows the normalized TOF distributions for $D(^2S)$ and $O(^3P_2)$ at several incident electron energies. [Similar TOF distributions have also been measured for the $O(^3P_1)$, $O(^3P_0)$, and $O(^1D_2)$ desorbates.] The peaks of the TOF distributions correspond to a translational energy of ~85 meV for $D(^2S)$ and ~60 meV for $O(^3P_2)$ (assuming negligible time delay between the incident electron pulse and the desorption of the neutral atoms). The peaks at short times in the TOF distributions are nonthermal components which are due to atoms ejected directly from the surface without interacting with surrounding molecules. The shoulders starting at ~3 and 10 μsec for the $D(^2S)$ and $O(^3P_2)$, respectively, also have contributions from atoms which have accommodated to the surface temperature prior to desorption. The Boltzmann TOF distributions expected for atoms accommodated to the surface temperature (88 K) are shown for comparison. The $O(^3P_0)$ and $O(^1D_2)$ velocity distribu-

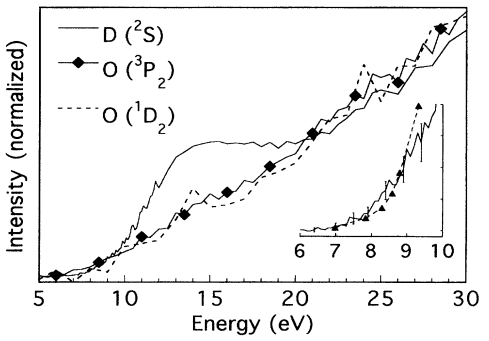

FIG. 2. $D(^2S)$, $O(^3P_2)$, and $O(^1D_2)$ intensities vs electron energy. The $D(^2S)$ yield rises rapidly above threshold and is constant from ~14 to 20 eV. The $O(^1D_2)$ and $O(^3P_2)$ have similar thresholds but increase more slowly above threshold. Inset: two-photon photoionization efficiency of liquid water [23] (triangles) compared to the $D(^2S)$ (solid line) threshold at ~6.5 eV. Error bars for the $D(^2S)$ data in the threshold region are indicated.

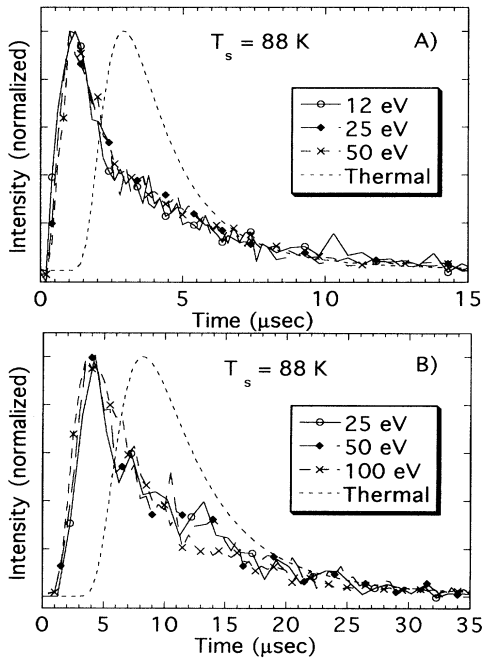

FIG. 3. Time-of-flight distributions for $D(^2S)$ and $O(^3P_2)$. The distributions, which have been normalized at the peak, have the same shape independent of the incident electron energy. (A) TOF distributions for $D(^2S)$. The peak of the TOF distributions corresponds to an energy of ~85 meV. (B) TOF distribution for $O(^3P_2)$. The peak of the TOF distributions corresponds to an energy of ~60 meV.

tions are also peaked at ~60 meV and contain only a minor thermal component as compared to the $O(^3P_2)$ TOF distribution. The ratios of the (nonthermal) peak intensities for the $O(^3P_J)$ are approximately 5.0:2.0:0.7 for $J = 2{:}1{:}0$, respectively, which is somewhat different than the high temperature (statistical) occupancy of 5:3:1.

In the gas phase, the lowest-energy excited states of water, the $^{1,3}B_1$ and the $^{1,3}A_1$ states, are dissociative. The production of $D(^2S)$ via photodissociation and electron-impact dissociation, $D_2O^* \rightarrow D(^2S) + OD(\tilde{X}\,^2\Pi$ and/or $\tilde{A}\,^2\Sigma^+)$, has been studied in detail [16–18]. For polyatomic molecules, in addition to simple dissociation, more complicated decay channels for the excited states, such as molecular elimination, are also possible. For example, the excited states of water can also decay to form $D_2(^1\Sigma_g^+) + O(^3P_J)$ or $D_2(^1\Sigma_g^+) + O(^1D_2)$ [19]. In the condensed phase, it is known that the dissociation of excited states (which can be described as excitons) can lead to the desorption of neutral fragments [13]. For ice, the very low threshold energies for the production of $D(^2S)$, $O(^3P_J)$, and $O(^1D_2)$ demonstrate that excitons, similar to the valence excited states in the gas phase, are important in the ESD of neutral fragments. The pathway for $D(^2S)$ desorption probably involves $D_2O^* \rightarrow D + OD$. However, an important observation is that the thresholds for producing $O(^3P_J)$ and $O(^1D_2)$, which are the same within experimental error (~6–7 eV), are *lower* than the 9.5 and 11.5 eV thermodynamic energies required to produce $O(^3P_J) + 2D(^2S)$ and $O(^1D_2) + 2D(^2S)$, respectively. The low threshold values therefore indicate that formation of $O(^3P_J)$ and $O(^1D_2)$ must occur by a pathway which involves simultaneous formation of D_2, i.e., via molecular elimination as discussed above. We have previously reported that the threshold for the production of D_2 from D_2O ice is also ~6–7 eV [5], supporting this conclusion.

Optical [20] and inelastic electron scattering [21] studies of amorphous and crystalline ice have identified excitons at ~8.6, 10.4, and 14.5 eV. The 8.6 eV exciton lies just below the conduction band edge and is the most clearly resolved in the optical studies. It has been assigned to the $1b_1 \rightarrow 3s4a_1$ ($^{1,3}B_1$) transition. The 10.4 and 14.5 eV excitons, which are in the conduction band, have been assigned to the $3a_1 \rightarrow 3s4a_1$ ($^{1,3}A_1$) and $1b_2 \rightarrow 3s4a_1$ ($^{1,3}B_2$) transitions, respectively. The forces in these excited states are due primarily to the antibonding nature of the $4a_1$ component of the mixed $3s4a_1$ band and should not depend strongly on the electronic structure of the "core" electrons.

As the incident electron energy increases above threshold, excitation of the different valence levels of the water molecules can occur; the total excitation cross section increases and the desorption yields increase (Figs. 1 and 2). In addition, the formation of multihole excited states is energetically allowed above ~21 eV [4]. Despite the new excitation channels, the shapes of the TOF distributions of the desorbing neutrals *do not change* as E_i increases (Fig. 3). In other words, the forces in the final states, which lead to dissociation and fragment desorption, are *independent* of the initial excitation. This suggests that most higher-energy excitations either autoionize or relax to the excited states near the bottom of the conduction band prior to dissociation. However, due to the large band gap in ice, the energy of these low lying electronically excited states cannot be effectively dissipated except via dissociation. Therefore, since the longest lived excited states usually dominate the desorption yield, the dissociation of these low-energy excitons is primarily responsible for the desorption of the atomic species from D_2O ice. This behavior is quite different from what is typically observed in the ESD of ions. For example, in the ESD of H^+ from ice, the ~21 eV threshold is attributed to the formation of multielectron (two-hole) states, and the desorbing protons have kinetic energies ranging from ~1 to 9 eV [4]. These kinetic energy distributions also shift to higher energy and become bimodal as E_i increases [4].

While the TOF distributions (Fig. 3) implicate low-energy neutral excited states as the *final* states leading to desorption of $D(^2S)$, $O(^3P_J)$, and $O(^1D_2)$, they do not indicate what (if any) intermediate steps occur prior to the formation of these states. Some possibilities include: (1) direct excitation to the dissociative states, (2) excitation of higher-energy neutral states which relax to the dissociative states, and (3) ionization (or autoionization of highly excited states) followed by recombination with quasifree trapped electrons to form the dissociative states. Direct excitation to the dissociative states, process (1), is likely to be most important in the threshold region, but less important at higher energies where the probability for excitation of these low-energy states should decrease. While excited states and resonances have been observed in photon-stimulated desorption from condensed O_2 [22], as well as electron energy loss spectroscopy [21] and dissociative electron attachment [3], studies of H_2O ice, the $D(^2S)$, $O(^3P_J)$, and $O(^1D_2)$ desorption yields (Figs. 1 and 2) show no discernible structure associated with such states at any energy. Since relaxation (either radiative or nonradiative) and autoionization rates are not well known for amorphous ice, it is difficult to assess the relative importance of processes (2) and (3). However, since both relaxation and autoionization followed by recombination lead to similar low-energy dissociative states, excitation of high-energy states is important as an initial step in the desorption process.

Since the *increase* in the desorption yields with E_i is closely related to the increasing number of ionizations and electronic excitations caused by the electron, it would be useful to compare the desorption yields with the electron-impact ionization or excitation efficiency of amorphous ice. Although this information is unavailable over this energy range, the photoionization yield of liquid water has been measured in the threshold region [23]

and calculated for $E_i \leq 100$ eV [24]. For condensed water, the onset of ionization does not have a distinct threshold but rather an approximately exponential tail, which extends to ~6.5 eV [23] and is quite similar to the $D(^2S)$ yield versus energy (Fig. 2, inset). This suggests that in the threshold region, dissociation and autoionization occur via similar intermediate states. The photoionization yield, like the $D(^2S)$ yield, increases rapidly above threshold, and has a plateau from ~15 to 21 eV and an approximately linear increase at higher energies [24]. For $\sim 14 \leq E_i \leq 21$ eV, the probability that an incident electron ionizes or electronically excites one substrate water molecule is constant (and equal to one for sufficiently thick ice layers), resulting in the plateau in the $D(^2S)$ yield (Fig. 2). Above ~21 eV, the desorption yield increases again since the electron has enough energy to ionize or excite two or more molecules. Also for $E_i > 21$ eV, the excitation of two-hole states [4] (followed by recombination and/or relaxation) may contribute to the neutral desorption yields.

These results on the stimulated desorption of amorphous ice are consistent with previous work on electron irradiation ($E_i \geq 200$ eV) of condensed N_2, NO, and O_2 which reported relatively low neutral kinetic energy (< 1 eV) distributions [13]. The present results support the suggestion by Hudel, Steinacker, and Feulner [13] that collision cascades initiated by energetic fragments from condensed phase electron-ion recombination are unlikely to result in desorption from molecular solids. The current results, as well as a previous study which reported substantial vibrational and rotational excitation in the desorbing D_2 products [6], suggest that desorption occurs primarily due to the dissociation of low-energy excitons. Inelastic scattering of the excited fragments also occurs, leading to the production of thermalized species which can subsequently desorb. Future investigations of the relative importance of ionization, followed by electron-ion recombination versus direct excitation of excited states in the desorption of neutrals from molecular solids are planned.

The authors gratefully acknowledge Dr. Bruce Kay, Dr. Russ Tonkyn, and Dr. Steve Joyce for useful comments and discussions. This work was supported by the Office of Basic Energy Sciences, Division of Chemical Sciences. Pacific Northwest Laboratory is a mulitprogram National Laboratory operated for the Department of Energy by Battelle Memorial Institute under Contract No. DE-AC06-76RLO-1830.

*To whom correspondence should be addressed.

[1] E. Mayer and R. Pletzer, Nature (London) **319**, 298 (1986).
[2] P. Jenniskens and D. F. Blake, Science **265**, 753 (1994).
[3] P. Rowntree, L. Parenteau, and L. Sanche, J. Chem. Phys. **94**, 8570 (1991).
[4] J. O. Noell, C. F. Melius, and R. J. Stulen, Surf. Sci. **157**, 119 (1985).
[5] G. A. Kimmel, T. M. Orlando, C. Vezina, and L. Sanche, J. Chem. Phys. **101**, 3282 (1994).
[6] G. A. Kimmel, R. G. Tonkyn, and T. M. Orlando, Nucl. Instrum. Methods Phys. Res., Sect. B **101**, 179 (1995).
[7] A. Kouchi and T. Kuroda, Nature (London) **344**, 134 (1990).
[8] M. S. Westley, R. A. Baragiola, R. E. Johnson, and G. A. Baratta, Nature (London) **373**, 405 (1995).
[9] W. L. Brown *et al.*, Phys. Rev. Lett. **45**, 1632 (1980).
[10] W. L. Brown, L. J. Lanzerotti, and R. E. Johnson, Science **218**, 525 (1982).
[11] A. R. Burns, Phys. Rev. Lett. **55**, 525 (1985).
[12] A. R. Burns, D. R. Jennison, E. B. Stechel, and Y. S. Li, Phys. Rev. Lett. **72**, 3895 (1994).
[13] E. Hudel, E. Steinacker, and P. Feulner, Surf. Sci. **273**, 405 (1992).
[14] L. Sanche, in *Desorption Induced by Electronic Transitions: DIET V,* edited by A. R. Burns, E. B. Stechel, and D. R. Jennison (Springer-Verlag, New York, 1992), p. 3.
[15] D. E. Ramaker, Chem. Phys. **80**, 183 (1983).
[16] C. R. Claydon, G. A. Segal, and H. S. Taylor, J. Chem. Phys. **54**, 3799 (1971).
[17] M. Brouard, S. R. Langford, and D. E. Manolopoulos, J. Chem. Phys. **101**, 7458 (1994).
[18] R. J. Sension, R. J. Brudzynski, and B. S. Hudson, Phys. Rev. Lett. **61**, 694 (1988).
[19] G. Theodorakopoulos, C. A. Nicolaides, R. J. Buenker, and S. D. Peyerimhoff, Chem. Phys. Lett. **89**, 164 (1982).
[20] K. Kobayashi, J. Phys. Chem. **87**, 4317 (1983).
[21] M. Michaud, P. Cloutier, and L. Sanche, Phys. Rev. A **44**, 5624 (1991).
[22] G. Dujardin *et al.*, Phys. Rev. Lett. **67**, 1844 (1991).
[23] D. N. Nikogosyan, A. A. Oraevsky, and V. I. Rupasov, Chem. Phys. **77**, 131 (1983).
[24] S. M. Pimblott and A. Mozumder, J. Phys. Chem. **95**, 7291 (1991).